Pergamon

Cement and Concrete Research 32 (2002) 247–252

CEMENT AND CONCRETE RESEARCH

Fracture energy and softening behavior of high-strength concrete

G. Appa Rao*, B.K. Raghu Prasad

Department of Civil Engineering, Indian Institute of Science, Bangalore 560 012, India

Received 20 September 2000; accepted 20 August 2001

Abstract

An experimental investigation on the fracture properties of high-strength concrete (HSC) is reported. Three-point bend beam specimens of size $100 \times 100 \times 500$ mm were used as per RILEM-FMC 50 recommendations. The influence of maximum size of coarse aggregate on fracture energy, fracture toughness, and characteristic length of concrete has been studied. The compressive strength of concrete ranged between 40 and 75 MPa. Relatively brittle fracture behavior was observed with the increase in compressive strength. The load–CMOD relationship is linear in the ascending portion and gradually drops off after the peak value in the descending portion. The length of the tail end portion of the softening curve increases as the size of coarse aggregate increases. The fracture energy increases as the maximum size of coarse aggregate and compressive strength of concrete increase. The characteristic length of concrete increases with the maximum size of coarse aggregate and decreases as the compressive strength increases. © 2002 Elsevier Science Ltd. All rights reserved.

Keywords: Aggregate; Concrete; Compressive strength; Fracture toughness; Silica fume

1. Introduction

The fracture energy, G_f, is one of the important material properties for the design of large concrete structures. In the fictitious crack model proposed by Hillerborg et al. [1] and Hillerborg [2,3], the fracture energy, G_f, tensile strength, f_t, and the stress–CMOD relationship completely describe the fracture characteristics of concrete. RILEM [4,5] and Petersson [6] recommended a method for the determination of G_f using simple three-point bend beam specimens. The fracture energy, G_f, is defined as the area under the load–deflection curve per unit fractured surface area. Hillerborg [7] concluded that there is a tendency for G_f to increase when the maximum aggregate size increases from 8 to 20 mm. Walsh [8] and Bazant and Oh [9] also reported the same tendency with increasing aggregate size. However, Zhou et al. [10] reported that the fracture energy increases with increasing aggregate size and stiffness, and that critical stress intensity factor, K_{Ic}, increases with increasing compressive strength. Giaccio et al. [11] reported that the fracture energy, G_f, of concrete increases with increase in the size of aggregate and strength of concrete, the displacements at peak load being dependent on the type and size of aggregate. The characteristic length, l_{ch}, decreases as the concrete strength increases. Petersson [12] reported that the fracture energy does not seem to be affected by the maximum particle size, while l_{ch} increases with increasing maximum particle size. The fracture surfaces are smooth and less tortuous in high-strength concrete (HSC) containing silica fume [13]. It has been reported that the fracture energy decreases and the brittleness index increases significantly with the incorporation of large size aggregate [14]. The type of fine aggregate has no influence on the fracture energy of concrete [15]. However, Barr et al. [16] and Barr and Hasso [17] reported that the fracture toughness was independent of the size of aggregate from beam specimens, while the highest toughness values were observed with 10-mm aggregate and the lowest with 20-mm aggregates from compact tension specimens. It seems that the influence of the maximum size of the aggregate has not been clearly understood, particularly so in HSC.

2. Experimental program

2.1. Materials

Grade 43 Portland cement conforming to IS: 8112-1989 was used for the program. Silica fume with 93.6% SiO_2 was used as a partial replacement material at 10% by weight of

* Corresponding author. Department of Civil Engineering, College of Engineering, Sri Venkateswara University, Tirupati, AP-517 502, India. Tel.: +91-8574-48261.

E-mail address: gangolu@civil.iisc.ernet.in (G.A. Rao).

0008-8846/02/$ – see front matter
PII: S0008-8846(01)00667-6

binder. The fine aggregate was natural river sand passing through a 2.36-mm sieve. Its specific gravity was 2.72 and the density was 1590 kg/m^3. The coarse aggregate used was crushed white granite with different maximum sizes of 4.75, 6.3, 12.5, and 20 mm. Potable water with high-range water-reducing agent (HRWRA) was used.

2.2. Test specimen: preparation and testing

Initially, the dry materials were thoroughly mixed in the required proportions. Water with HRWRA was then added and the concrete was mixed up to a uniform stage. Subsequently, the fresh concrete was poured into the beam moulds prepared by placing steel channels back to back with the required beam depths. A plate vibrator was used to compact the concrete in the moulds in three layers. Twenty-four hours after casting, the specimens were demoulded and cured in water for 28 days, with the ambient climatic conditions of 27 ± 2 °C temperature and 65 ± 5% relative humidity. The specimens were taken out from the curing tanks after 28 days and then central notches were made using a diamond saw. The size of the TPB specimens was 100 × 100 × 500 mm, with an effective span of 400 mm and a notch-to-depth ratio of 0.50.

Specimens were tested under three-point bending employing load-controlled universal testing machine. The stiffness of the testing machine was larger than that of the test specimen. By carefully operating the loading machine, the postpeak response was obtained. The load was applied with very slow rate of loading up to the peak load and then the pressure valve was slightly closed to achieve stable crack propagation in the beams. It was possible to achieve the postpeak response, i.e., softening branch of load–CMOD curve even with an ordinary load-controlled machine. In this case, load–CMOD variations were used to evaluate the fracture properties. In order to account for the difference in the fracture energy between load–deflection and load–CMOD variations, a correction factor has been adopted [23]. The correction factor in the present case is 0.815 (for $a/d = 0.5$ and $l/d = 4.0$).

2.3. Mix proportioning

Four maximum sizes of coarse aggregate namely 4.75, 6.3, 12.5, and 20 mm have been used. A constant water-to-cement ratio of 0.325 with a naphthalene sulphonate-type superplasticizer (Complast SP 430) at 5.0 l/m^3 of concrete was used. Table 1 shows various quantities of constituent materials of the concrete mixes. Silica fume was used as partial replacement material at 10% by weight of binder.

3. Test results and discussion

The influence of maximum size of coarse aggregate on fracture energy, fracture toughness, and characteristic length of concrete has been studied using three-point bend beam test specimens.

3.1. Fracture energy

Table 2 shows the mechanical and fracture properties of the various concrete mixes. The compressive strength of concrete varied between 40 and 75 MPa. The compressive strength of concrete increases as the maximum size of coarse aggregate increases. Fig. 1 shows the variation of compressive strength with maximum size of coarse aggregate in medium to HSC, with and without silica fume. A similar trend has also been observed in the case of splitting tensile strength. From the experimental test results, it has been noticed that the modulus of elasticity of concrete slightly increases as the maximum size of coarse aggregate increases. This is due to the addition of stiffer aggregate particles, which have increased the stiffness of the product. The modulus of elasticity was determined using the ultrasonic pulse velocity technique. The fracture energy, G_f, of concrete was 76.6 N/m in concrete with smaller maximum size of coarse aggregate equal to 4.75 mm. The fracture energy increased to 142 N/m in concrete with maximum size of coarse aggregate equal to 20 mm in plain concrete. The fracture energy increased from 122 to 165 N/m in

Table 1
Mix proportioning of concrete mixes with and without silica fume

Mix designation	Size of aggregate (mm)	Cement (kg/m^3)	Silica fume (kg/m^3)	Sand (kg/m^3)	Coarse aggregate (kg/m^3)	Super plasticizer (l/m^3)	Water content (l/m^3)	Water-to-binder ratio
HPC-4.75	4.75	450	00.00	700	900	5.00	146	0.325
HPC-6.3	6.30	450	00.00	700	900	5.00	146	0.325
HPC-12.5	12.50	450	00.00	700	900	5.00	146	0.325
HPC-20	20.00	450	00.00	700	900	5.00	146	0.325
HSFC-4.75	4.75	405	45.00	700	900	5.00	146	0.325
HSFC-6.3	6.30	405	45.00	700	900	5.00	146	0.325
HSFC-12.5	12.50	405	45.00	700	900	5.00	146	0.325
HSFC-20	20.00	405	45.00	700	900	5.00	146	0.325

Mix proportions: binder/water/fly ash/coarse aggregate = 1:0.325:1.56:2.00.

Table 2
Mechanical and fracture properties of concrete with various coarse aggregate sizes

Mix designation	Compressive strength (MPa)	Tensile strength (MPa)	Modulus of elasticity (GPa)	Fracture energy (N/m)	Fracture toughness (MPa$\sqrt{m}$)	Characteristic length (mm)	
						l_{ch}	$l_{ch,mod}$
HPC-4.75	40	2.39	37.24	76.6	1.69	500	29.8
HPC-6.3	57.8	2.7	39.5	97.8	1.97	532	24.8
HPC-12.5	58.7	2.9	39.67	103	2.02	489	24.0
HPC-20	61	3.06	42.11	142	2.47	649	32.0
HSFC-4.75	55	2.55	39.5	122	2.19	742	34.3
HSFC-6.3	63	3.31	40.2	137	2.34	503	26.43
HSFC-12.5	75	4.01	42.1	151	2.52	394	21.10
HSFC-20	74	3.8	42.9	165	2.62	478	24.53

concrete with silica fume. As observed in Table 2, the fracture energy increases as the maximum size of coarse aggregate increases. The increase of fracture energy with the maximum size of coarse aggregate or size of nonhomogeneity in the concrete may be in part attributed to increased aggregate interlock. As the size of coarse aggregate increases, the cement paste–aggregate interface experience higher bond stresses leading to bond failure. Whereas in the case of concrete mixes with smaller size coarse aggregate, the bond stress at the interface is less due to the higher specific surface area of the aggregate. Therefore, aggregate–matrix interface failures are less likely in concretes with smaller size of aggregates compared to concrete with larger size of aggregates. Therefore, the crack path is more tortuous in concrete with large size aggregates. A more tortuous crack results in increased fracture energy. The composite behavior of HSC has been reported to be enhanced with increasing compressive strength [18].

Fig. 2 shows the variation of fracture energy with the maximum size of coarse aggregate. As has been shown, in concrete mixes with and without silica fume, the fracture energy increases as the maximum size of coarse aggregate increases. The addition of 10% silica fume has improved the strength of concrete very significantly. However, the information in the literature reveals that the optimum content of

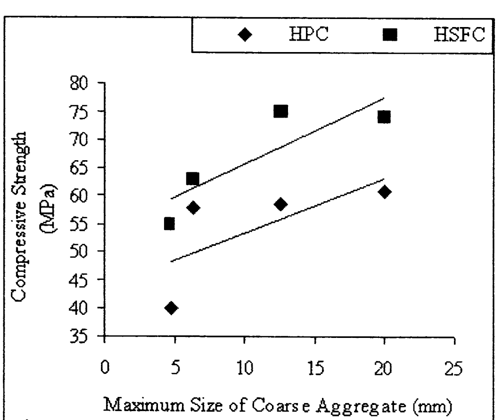

Fig. 1. Variation of compressive strength with maximum size of coarse aggregated in HPC and HSFC.

silica fume is approximately 15–20% by weight of cement. Further, the fracture energies of silica fume concrete were higher than those of plain concrete [14]. The fracture energy, G_f, of HSC appears to be increased as the maximum size of coarse aggregate increases. It has been reported that the fracture energy increases with the maximum size of coarse aggregate with single size aggregate, but the increase has been observed to be very significant with the combination of different sizes of coarse aggregate sizes. At the aggregate size of 20 mm, the fracture energy seems to be very significant [19]. Longer descending portions of the load–CMOD diagrams have been observed in concrete mixes with larger size coarse aggregate. Further, it has been observed that the concrete mixes with larger size coarse aggregate exhibited few traces of pulling out of the aggregate from the matrix.

Fig. 3 shows the variation of fracture energy with the compressive strength of concrete. Fracture energy increases as the compressive strength increases. In HSC, the total energy could be considered to be utilized in two forms [19,24]. The first form of energy seemed to be utilized energy in overcoming the surface forces of concrete (surface energy), while the second form of fracture energy seemed to be utilized in overcoming the cohesive forces due to aggregate bridging, aggregate interlocking, friction forces, and other mechanisms in the fracture process zone. It has been reported that the interface between cement paste with silica fume and aggregate is very strong and the concrete behaves more like a composite material. The postpeak response seems to be steep with increase in the strength of concrete. This process results in the catastrophic behavior of HSC. Due to strong interface, the process zone in front of the initial crack tip localizes resulting in the decrease in the absorption of fracture energy in this zone.

3.2. Fracture toughness

The fracture toughness of concrete, with different maximum sizes of coarse aggregate, has been studied. The critical stress intensity factor, K_{Ic}, has in the past been used to represent the fracture toughness, although today its use is generally restricted to brittle high-strength cementitious pastes. Fig. 4 shows the variation of the apparent fracture toughness with maximum size of coarse

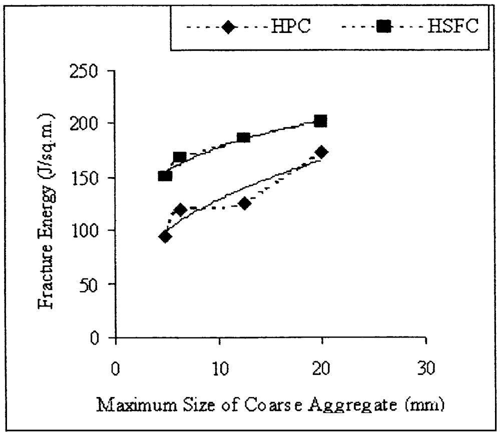

Fig. 2. Variation of fracture energy with maximum size of coarse aggregate in HPC and HSFC.

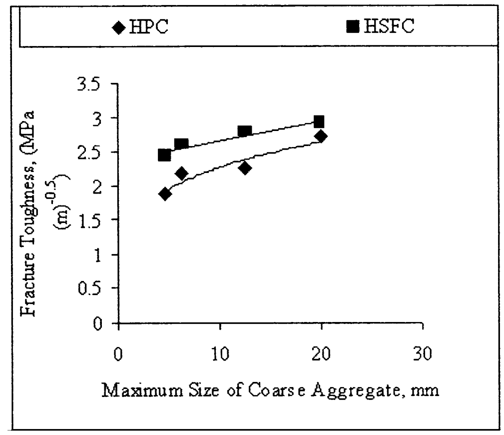

Fig. 4. Variation of fracture toughness with maximum size of coarse aggregate in HSC.

aggregate. It indicates that the apparent fracture toughness increases as the maximum size of coarse aggregate increases. The same reasons outlined for the variation of fracture energy are also mainly responsible for the variation of fracture toughness. This could be attributed again, to the fact that the larger size aggregate particles induce more aggregate interlock. At higher stress levels, at the interface between cement paste and aggregate, due to the difference in stiffness of aggregate and cement paste, stress concentration takes place since the aggregates act as discontinuities in the concrete. The results are found to coincide with the reports on fracture behavior of HSC by Giaccio et al. [11], Zhou et al. [10], and Kim et al. [15]. But Barr et al. [16] Barr and Hasso [17] reported different variations of test results from their studies on the influence of coarse aggregate on fracture energy and fracture toughness of concrete with different types of specimens.

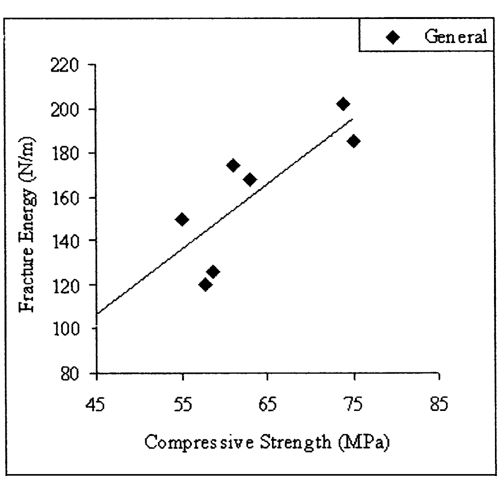

Fig. 3. Variation of fracture energy with compressive strength in HSC.

3.3. Characteristic length

The brittleness of concrete has been evaluated by a parameter called characteristic length, $l_{ch} = EG_f/f_t^2$. The values of characteristic length from the different concrete mixes are shown in Table 2. Using the characteristic length equation, the values are observed to be very high, but similar to those in the literature. In the case of plain concrete without silica fume, the characteristic length increases as the maximum size of coarse aggregate increases, which indicates increased ductility. While in concrete containing silica fume, the characteristic length decreases up to an aggregate size of 12.5 mm, after that it increases. The influence of maximum size of coarse aggregate has been investigated on the characteristic length of concrete. It has been observed that the characteristic length of concrete increases as the maximum size of coarse aggregate increases. Tasdemir et al. [14] reported similar conclusions for concrete mixes without silica fume. It has also been reported that in HSC, the characteristic length values are two to three times smaller than those obtained in conventional concrete [11]. However, the specimens made from concrete containing larger size coarse aggregate particles showed a more tortuous fracture path. Whereas in concrete with smaller size coarse aggregate, the fracture surface was observed to be relatively smooth.

In the case of HSC, the measure of brittleness using characteristic length expression does not contain a very important parameter, i.e., compressive strength. An effort has been made in this study to investigate the influence of various factors on the characteristic length of concrete. Using dimensional analysis, the characteristic length of HSC has been investigated. A modified characteristic length, which incorporates the compressive strength of concrete also, has been developed. From dimensional analysis, a modified form of the characteristic length may be given by $l_{ch,mod} = EG_f/f_c f_t$. The modified characteristic length of concrete decreases as the brittleness increases.

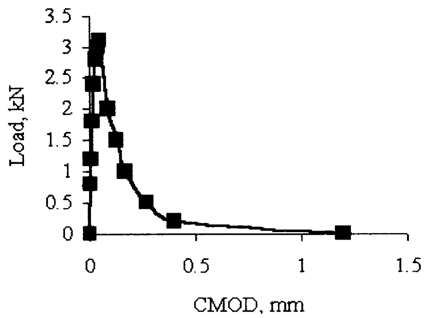

Fig. 5. Typical graph showing the variation of load with CMOD in HSC.

The reason for the decrease in the characteristic length seems to be the strengthening mechanism of the cement paste–aggregate interfacial bond. From the modified expression for the characteristic length, the experimental results fall in the range between 26 and 40 mm. It has been observed that the characteristic length decreases with the increase in the strength of concrete. However, some concrete mixes exhibited inconsistency in the variation of characteristic length.

From the variation of load versus crack mouth opening displacement curves, it has been generally observed that the postpeak response seems to be very gradual and the length of the tail end portion increases as the maximum size of coarse aggregate increases. This indicates that the ductility of concrete increases as the size of coarse aggregate increases. Further, it has been noticed that the ultimate load-carrying capacity increases as the maximum size of coarse aggregate increases. Fig. 5 shows a typical load–CMOD variation in HSC. The postpeak curve drops off steeply resulting in less energy absorption capacity. ACI Committee 363 [20] has shown typical stress–strain curves for normal-, medium-, and high-strength concrete. The stress–strain curves produced from other studies also showed similar trends to that observed in this study [18,21,22].

Fig. 5 shows the variation of load with CMOD in a typical concrete mix. The ascending part of the curve is more linear in HSCs. After the peak value, the curves drop off gradually until zero load is reached. The descending part of the stress–strain curve becomes steeper as the concrete strength increases. The tail of the descending branch is longer in the case of low-strength concretes and shorter in the case of HSCs. This indicates that toughness of the concrete decreases with strength. The crack mouth opening displacements at the ultimate load and postpeak zero loads have been observed. The magnitude of the CMOD at the ultimate load has been very small compared to the CMOD at the postpeak zero loads. The mean values of CMOD at the peak load ranges between 0.055 and 0.10 mm, while the CMOD at the postpeak zero loads ranged between 0.82 to 1.55 mm. This variation is reflected in the values obtained for l_{ch}.

4. Conclusions

The fracture energy, fracture toughness, and the characteristic length of HSC increase as the maximum size of coarse aggregate increases. The fracture energy increases as the compressive strength of concrete increases. Further, the characteristic length of concrete slightly decreases as the compressive strength increases. It has been generally observed that the ascending portion of the load–CMOD curve is linear up to about 90% of the peak load and it gradually drops off in the softening region. From the knowledge of the variation of load versus CMOD, the ductility of concrete, indicated by the extension of the tail end of the softening curve, increases with the maximum size of coarse aggregate.

References

[1] A. Hillerborg, M. Modeer, P.E. Petersson, Analysis of crack formation and crack growth in concrete by means of fracture mechanics and finite elements, Cem. Concr. Res. 6 (6) (1976) 773–782.
[2] A. Hillerborg, Analysis of one single crack, in: F.H. Wittmann (Ed.), Fracture Mechanics of Concrete, Elsevier, Amsterdam, 1983, pp. 223–249.
[3] A. Hillerborg, The theoretical basis of a method to determine the fracture energy G_F of concrete, Mater. Struct. 18 (106) (1985) 291–296.
[4] RILEM Draft Recommendation, 50-FMC committee fracture mechanics of concrete, Mater. Struct. 18 (106) (1985) 285–290.
[5] RILEM, in: S.P. Shah, A. Carpentari (Eds.), Fracture Mechanics Test Methods for Concrete (FMC 89), Chapman & Hall, London, 1990.
[6] P.E. Petersson, Fracture energy of concrete: Method of determination, Cem. Concr. Res. 10 (1) (1980) 79–89.
[7] A. Hillerborg, Results of three comparative test series for determining the fracture energy G_f of concrete, Mater. Struct. 18 (107) (1985) 33–39.
[8] P.F. Walsh, Fracture of plain concrete, Indian Concr. J. 46 (11) (1972) 469–476.
[9] Z.P. Bazant, B.H. Oh, Crack band theory for fracture of concrete, Mater. Struct. 16 (93) (1983) 155–177.
[10] F.P. Zhou, B.I.G. Barr, F.D. Lydon, Fracture properties of high strength concrete with varying silica fume content and aggregates, Cem. Concr. Res. 25 (3) (1995) 543–552.
[11] G. Giaccio, C. Rocco, R. Zerbino, The fracture energy of high strength concretes, Mater. Struct. 26 (1993) 381–386.
[12] P.E. Petersson, Fracture energy of concrete: Practical performance and experimental results, Cem. Concr. Res. 10 (1) (1980) 91–101.
[13] B.B. Sabir, S. Wild, M. Asili, On the tortuosity of the fracture surface in concrete, Cem. Concr. Res. 27 (5) (1997) 785–795.
[14] C. Tasdemir, M.A. Tasdemir, F.D. Lydon, B.I.G. Barr, Effects silica fume and aggregate size on the brittleness of concrete, Cem. Concr. Res. 26 (1) (1996) 63–68.
[15] J.K. Kim, C.S. Lee, C.K. Park, S.H. Eo, The fracture characteristics of crushed lime stone sand concrete, Cem. Concr. Res. 27 (11) (1997) 1719–1729.
[16] B.I.G. Barr, E.B.D. Hasso, V.J. Weiss, Effect of specimen and aggregate sizes upon the fracture characteristics of concrete, J. Cem. Compos. Lightweight Concr. 8 (2) (1986) 109–119.
[17] B.I.G. Barr, E.B.D. Hasso, Fracture toughness testing by means of the SECRBB test specimen, J. Cem. Compos. Lightweight Concr. 8 (1) (1986) 03–09.
[18] J. Xie, A.E. Elwi, J.G. Mac Gregor, Mechanical properties of three

high strength concretes containing silica fume, ACI Mater. J. 92 (2) (1995) 135–145.

[19] G.A. Rao, B.K. Raghu Prasad, Size effect and fracture properties of HPC, Proc. 14th Eng. Mech. Int. Conf. (ASCE), Austin, Texas, May 21–24, 2000, pp. 104.

[20] ACI Committee 363, State-of-the-art report on high-strength concrete, ACI Mater. J. ACI 363 R-84 (1984) 363–411.

[21] P.A.J. Gutierrez, M.F. Canovas, High performance concrete—requirements for constituent materials and mix proportioning, ACI Mater. J. 93 (3) (1996) 233–241.

[22] V. Novokshchenov, Factors controlling the compressive strength of silica fume concrete in the range 110–150 MPa, Mag. Concr. Res. 44 (158) (1992) 53–61.

[23] R.K. Navalurkar, C.T.T. Hsu, S.K. Kim, M. Wacharatna, True fracture energy of concrete, ACI Mater. J. 96 (2) (1999) 213–225.

[24] G.A. Rao, Nonlinear fracture and size effect in high strength and high performance concrete—An experimental approach, PhD thesis, Indian Institute of Science, Bangalore, India, 2001.